doi:10.3788/gzxb20134202.0127

Eu^{2+}-Yb^{3+}共掺磷酸盐玻璃中的合作能量传递

徐波,杨斌,张约品,王金浩,夏海平

(宁波大学 光电子功能材料重点实验室,浙江 宁波 315211)

摘 要:报道了在 Eu^{2+}-Yb^{3+}共掺磷酸盐中,一个紫外光子(320 nm)通过下转换发光变成两个近红外光子(约 1 000 nm)的现象.测试了不同样品的吸收、激发和发射光谱,证明了在本玻璃体系中量子剪裁现象的存在;Eu^{2+}离子 5d-4f 能级发光的衰减曲线证明 Eu^{2+}到 Yb^{3+}之间的合作能量传递;用 I-H 理论模型拟合衰减曲线说明了能量传递的过程.最后计算出了能量传递的效率,当 Yb^{3+}浓度为 1.0 mol%时效率为 23.05%,当其增加到 2.0 mol%时,能量传递效率提高到了53.6%.

关键词:能量传递;下转换;激发和发射;磷酸盐玻璃

中图分类号:O482.31 **文献标识码**:A **文章编号**:1004-4213(2013)02-0127-5

Cooperative Energy Transfer in Eu^{2+}-Yb^{3+} Codoped Phosphate Glasses

XU Bo, YANG Bin, ZHANG Yue-pin, WANG Jin-hao, XIA Hai-ping

(*Key Laboratory of Photo-electronic Materials, Ningbo University, Ningbo, Zhejiang* 315211, *China*)

Abstract: Downconversion luminescence of one UV photon (320 nm) cut into two near-infrared photons (around 1 000 nm) was reported in Eu^{2+}-Yb^{3+} co-doped phosphate glasses. Absorption, excitation and emission spectra were carried out to demonstrate the occurrence of quantum cutting in this system. The experimental evidences of the cooperative energy transfer from Eu^{2+} to Yb^{3+} were presented by the decay curves of 5d→4f emission of Eu^{2+} ions. Luminescence decay curves of Eu^{2+} emission were recorded as a function of the Yb^{3+} concentration and analyzed by using Inokuti-Hirayama's model for energy transfer. Energy transfer efficiency was also calculated to be 23.05% for the Eu^{2+}-1.0Yb^{3+} co-doped sample, and 53.6% increased for the Eu^{2+}-2.0Yb^{3+} co-doped sample.

Key words: Energy transfer; Downconversion; Excitation and emission; Phosphate glass

0 Introduction

Recently a new quantum cutting (QC) from photon shorter than 500 nm to two near-infrared photons through the approach of cross relaxation and energy transfer has been investigated in rare-earth co-doped systems, such as Tb^{3+}-Yb^{3+}[1-3], Tm^{3+}-Yb^{3+}[4-7], and Pr^{3+}-Yb^{3+}[8-9]. The Yb^{3+} ions has a relatively simple electronic structure of two energy-level manifolds: the $^2F_{7/2}$ ground state and $^2F_{5/2}$ excited state around 10 000 cm^{-1} in the NIR region. Yb^{3+} ions is an excellent acceptor and emitter for downconversion materials of c-Si solar cells due to its band emission from 900 to 1 100 nm which is just above the band gap of c-Si. However, Tb^{3+}, Tm^{3+}, and Pr^{3+} ions have narrow absorption linewidth and low absorption cross section for UV-visible photons due to the 4f-4f transition, which leads to narrow band excitation and weak NIR emission of Yb^{3+}. It is difficult to

Foundation item: The National Natural Science Foundation of China (Nos. 61275180, 50972061, 51272109), the Natural Science Foundation of Zhejiang Province (Nos. Z4110072, R4100364), the Opening Foundation of Zhejiang Provincial Top Key Discipline, and K. C. Wang Magna Fund in Ningbo University

First author: XU Bo (1987—), male, M. S. degree, mainly focuses on rare-earth doped materials for improving solar cells efficiency. Email: benevone@163.com

Corresponding author: ZHANG Yue-pin (1968—), male, professor, mainly focuses on photo-electronic materials. Email: zhangyuepin@nbu.edu.cn

Received: Sep. 24, 2012; **Accepted**: Nov. 19, 2012

use these downconversion materials to practical application because only a relatively small high energy part of the solar spectrum is used.

For the efficient spectral modification of solar cells, strong and broad absorption of solar energy is an important factor. Optical transitions of Eu^{2+} in the UV to visible regions are due to allowed f-d transitions. As a result, the absorption linewidth and cross sections are wide and large, respectively. In addition, the emission spectra due to the f-d transition of Eu^{2+} ions are also usually broadened because of the large spatial extension of the 5d wave function. The emission due to 5d-4f transition and $^6P_{7/2}$-$^8S_{7/2}$ transition of Eu^{2+} ions are strongly influenced by the glass host. The phosphate glass is chosen to be the host for europium ions because of high solubility for rare earth elements which allows the high Eu^{2+} ion concentration in the glass. So Eu^{2+}/Yb^{3+} codoped systems may be a pair of donor and acceptor which can convert the high-energy photons to NIR photons.

In this work, we prepared Eu^{2+} ions doped glasses using aluminium powder as a strong reducing agent. The dependence of the Yb^{3+} doping concentration on the visible and NIR emissions, decay lifetimes, and energy transfer efficiency from Eu^{2+} to Yb^{3+} were investigated. Based on the decay curves, Inokuti-Hirayama′s model was used to analyze energy transfer mechanism between Eu^{2+} and Yb^{3+}, proving that the energy transfer of the electric dipole-dipole interaction is dominant in this system.

1 Experimental

Glasses with the same matrix of $50P_2O_5$-$45BaO$-$5Al_2O_3$ doped with the following composition in mol%: $0.5Eu_2O_3$ and xYb^{3+} (x=0, 1.0, 2.0) were prepared by the melting-and-quenching method using high purity of $NH_4H_2PO_4$, $BaCO_3$, $Al(OH)_3$, Eu_2O_3 and Yb_2O_3 as raw materials. Then aluminium powder used with the same weight in all samples was completely mixed with the chemical agents. The batches of 25 g were mixed homogeneously and melted in an Al_2O_3 corundum crucible under air atmosphere. After keeping at 1 350℃ for 30 min, the glass melt was poured into a stainless steel plate. The cooling rate was estimated at about 10 ℃/s. Each glass was annealed for 2 hours at 480 ℃ and cooled to room temperature slowly. Transparent light-yellow glasses were obtained herein. The samples were cut into small pieces with thickness of 2 mm and well polished. The absorption spectra were measured with Perkin-Elmer Lamda35 UV/VIS spectrophotometer, while the emission spectra, excitation spectra, and the fluorescence decay curves were recorded with a Hitachi F-4500 Fluorescence spectrophotometer with a resolution of 1 nm. All the measurements were carried out at room temperature.

2 Results and discussion

Fig. 1 shows the absorption spectra of samples doped Eu^{2+}-xYb^{3+} (x= 0, 1.0, and 2.0) ranging from 300 nm to 1 100 nm. There are two strong absorption bands centered in the UV and NIR regions, respectively. The strong and broad absorption band of Eu^{2+} ions in UV-visible region due to 4f-5d transitions may enhance the efficient spectral modification of solar cells. In the UV regions, the absorption band peaking at 320 nm in Eu^{2+} simply doped sample can be ascribed to be charge transfer state of Yb^{3+}, while the absorption band peaking at 342 nm in Eu^{2+}/Yb^{3+} co-doped samples due to the transition of Eu^{2+}: $4f^7 \rightarrow 4f^6 5d$, which has been reported by Zhou *et al*. in literature [10]. In addition, when the Yb^{3+} doped, the absorption edge shifts to long wavelength, which must be ascribed to the charge transfer transition of Yb^{3+}, involving transfer of an electron from the surrounding $2p^6$ orbital of O^{2-} to the $4f^{13}$ orbital of Yb^{3+}[11]. In the NIR region, it is worth noting that the strong absorption band assigned to the Yb^{3+} : $^2F_{5/2} \rightarrow {}^2F_{7/2}$ transition can be clearly observed in the wavelength range from 900 ~ 1 100 nm[3]. The absorption strength of Yb^{3+} transition around 1 000 nm increases with increasing Yb^{3+} concentration.

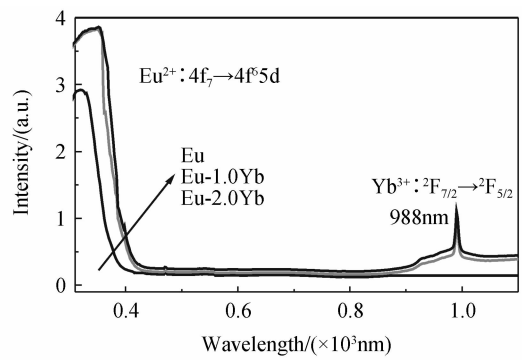

Fig. 1 The absorption spectra of samples: Eu^{2+}, Yb^{3+} (0%, 1.0%, and 2.0%)

Fig. 2 depicts the excitation and emission spectra of all studied samples. In PLE spectra, the

excitation band corresponding to Eu^{2+}: 454 nm emission is situated at 392 nm, which can be assigned to 4f→5d transition. In Eu^{2+}-2.0Yb^{3+} co-doped sample, a weaker band is observed at 392 nm by monitoring $^2F_{5/2}$ →$^2F_{7/2}$ transition of Yb^{3+} at 980 nm emission. The observation of Eu^{2+}: $4f^65d^1$ → $4f^7$ lines in the excitation of Yb^{3+} shows that the ET from Eu^{2+} to Yb^{3+} is present. Excitation at 320 nm lights gives rise to emission spectra as shown in right side of Fig. 2. The luminescence spectra consisted of a broad band from 400 to 570 nm centred at 454 nm which could be ascribed to the $4f^65d$ → $4f^7$ transition of Eu^{2+} ions and some sharp emission peaks corresponding to the transitions of the excited $^5D_0$ energy level to $^7F_1$(589 nm), $^7F_2$(612 nm), $^7F_3$(653 nm), $^7F_4$ (701 nm) levels of Eu^{3+} ions. However, it is easy to find that the emission intensity of Eu^{3+} at above four peaks almost have no change when doping Yb^{3+} ions, while that of Eu^{2+} at 454 nm decreases obviously. That is to say that there is no effect for Eu^{3+} ions to change the NIR luminescence from Yb^{3+}, and we focus on discussing the energy transfer from Eu^{2+} to Yb^{3+} ions in this system. Yb^{3+} emission in the wavelength range of 950 ~ 1100 nm is observed due to excitation of 320 nm. Two peaks in the infrared region of Yb^{3+} emission can be found: a sharper peak located at 973 nm and a broader peak centered at 1008 nm. However, for the Eu^{2+} singly doped sample, no emissions in the NIR region are detected. These results indicate that energy transfer from Eu^{2+}: $4f^65d^1$ to Yb^{3+}: $^2F_{5/2}$ is the only possible relaxation route to achieve NIR emission because Yb^{3+} has no other levels up to the UV region.

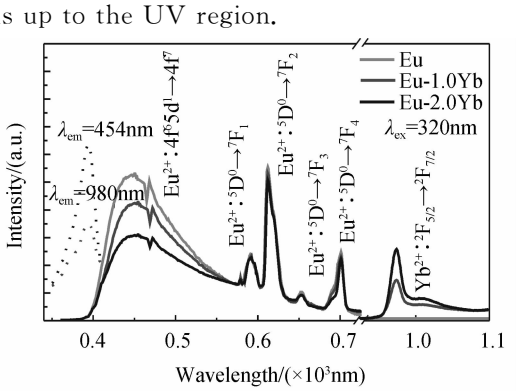

Fig. 2　The excitation spectra of Eu^{2+} 454 nm emission monitored in Eu^{2+} singly doped sample and of Yb^{3+} 980 nm emission monitored in Eu^{2+}-2.0Yb^{3+} co-doped sample(left); the emission spectra of all studied samples under 320 nm excitation(right)

From the obtained emission spectrum, we can also estimate the impact of the concentration ratio of Yb^{3+} ions over Eu^{2+} ions on energy transfer efficiency (ETE). For the Eu^{2+} singly doped sample, there are no emissions in the NIR region, that is to say, the ETE is closed to 0. When Yb^{3+} concentration increases to 1.0 mol%, the emission intensity of Yb^{3+} in the NIR region increases while that of Eu^{2+} at 454 nm decreases, which enhances the corresponding ETE. When the ratio above increases once again, the emission intensity of Yb^{3+} is two times stronger than that of Eu^{2+}-1.0Yb^{3+} sample, and the ETE is much larger than that too. It is concluded that the increasing concentration ration can improve the energy transfer from Eu^{2+} to Yb^{3+} ions.

Fig. 3 presents the schematic energy levels with the transitions which may be involved in the energy transfer process from Eu^{2+} to Yb^{3+} ions. The first excited $4f^65d$ configuration of Eu^{2+} lies close to the excited $4f^7$ levels. The transitions between the first $4f^65d$ configuration and the $4f^7$ ground state are dipole allowed and give very intense emission intensity about 10^6 times those of the f-f transition in the trivalent ions.[12] After excitation of Eu^{2+}: $4f^65d^1$ level by 320 nm photons, as the energy of Eu^{2+}: $^4f^65d^1$ → $4f^7$ transition is approximately twice as that of Yb^{3+}: $^2F_{5/2}$ →$^2F_{7/2}$ transition, the excited Eu^{2+} ion transfers its part energy to two Yb^{3+} ions, and then Yb^{3+} ions emit two NIR photons. Since the Yb^{3+} ions has only one excited multiplet $^2F_{5/2}$ around 10 000 cm^{-1} and no transition from the Eu^{2+}: $^4f^65d^1$ level is situated at this energy, resonant ET from the $4f^65d^1$ state of Eu^{2+} to one Yb^{3+} is impossible. The mechanism responsible for downconversion can be proved as cooperative energy transfer not as energy transfer through cross relaxation. So an excitation with UV light in this system might exhibit a cooperative ET from Eu^{2+} to two Yb^{3+} ions: $4f^65d$→$^2F_{5/2}$ + $^2F_{5/2}$.

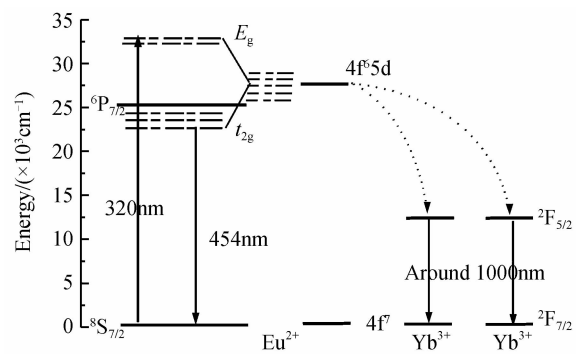

Fig. 3　The schematic energy level of Eu^{2+} and Yb^{3+} in glasses showing possible mechanism for NIR quantum cutting under excitation of UV with 320 nm

To get insight in the energy transfer

mechanism, we record luminescence decay curves for the Eu^{2+} emission. Fig. 4 (dots) shows the decay curves of $4f^6 5d^1 \rightarrow 4f^7$ emission of Eu^{2+} at 454 nm upon excitation at 320 nm. It can be seen that fluorescent intensity decays quickly in the co-doped samples because the energy transfer from Eu^{2+} to

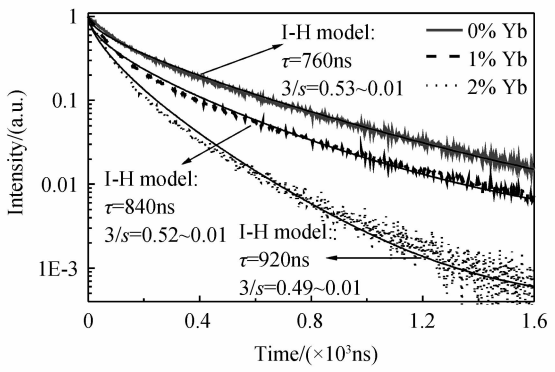

Fig. 4 Luminescence decay curves of the $4f^6 5d^1 \rightarrow 4f^7$ emission of Eu^{2+} at 454 nm

Yb^{3+} occurs. From the decay curves, the average fluorescent lifetimes can be calculated by using the following formula[13]

$$\bar{\tau} = \frac{\int I(t) t \mathrm{d}t}{\int I(t) \mathrm{d}t} \tag{1}$$

where $I(t)$ represents the luminescence intensity as a function of time t. The average lifetimes of $4f^6 5d^1$ for Eu^{2+}-$x$$Yb^{3+}$ (x=0, 1, 2) are 215, 131 and 84 ns, respectively. For 0 mol% Yb^{3+} concentration, the decay curve is close to single exponential with a 215 ns decay lifetime. And with the addition of Yb^{3+} content from 0 mol% to 2 mol%, the lifetimes decline from 215 ns to 84 ns, and the decay curves turn to be non-exponential, implying the introduction of efficient energy transfer from $4f^6 5d^1$ of Eu^{2+} to Yb^{3+} ions.

The experimental measured decay curves are simulated by following the Inokuti-Hirayama′s model [14] for energy transfer in Fig. 4

$$I(t) = I(0) \exp\left[-\frac{t}{\tau_0} - \frac{4\pi}{3}\Gamma\left(1-\frac{3}{s}\right) \cdot R_0^3 N \left(\frac{t}{\tau_0}\right)^{3/s}\right] \tag{2}$$

where s=6, 8, and 10, respectively, denote the electric dipole-dipole (Edd), dipole-quadrupole (Edq), and quadrupole-quadrupole (Eqq) interactions between luminescent centers, τ_0 is the intrinsic radiation lifetime, N is the concentration, R_0 is the critical transfer distance, and $\Gamma(1-3/s)$ is a Gamma function. By fitting the experimental fluorescent decay data to the I-H model, τ_0 and $3/s$ are obtained as shown in Fig. 4. These indicate the non-exponential fluorescent decays of co-doped samples obey the I-H model. From the fitting processes, the values of $3/s$ are 0.53, 0.52 and 0.49, that is to say that s is close to 6. Therefore, the energy transfer of Edd interaction is dominant in these samples.

From the fluorescent decay curves, the energy transfer efficiency (ETE) (η_{ETE}) can be determined. The energy transfer efficiency η_{ETE} is defined as the ratio of Eu^{2+} ions that depopulated by ET to Yb^{3+} ions over the total number of Eu^{2+} ions excited. η_{ETE} is obtained as a function of the Yb^{3+} concentration as follows[2]

$$\eta_{ETE} = \eta_{x\%\,Yb} = 1 - \frac{\int I_{x\%\,Yb} \mathrm{d}t}{\int I_{0\%\,Yb} \mathrm{d}t} \tag{3}$$

where I represents the intensity of 454 nm at time t and x% stands for the Yb^{3+} concentration. According to the fluorescent decay curves and Eq. (3), η_{ETE} for Eu^{2+}-$x$$Yb^{3+}$ (x = 0, 1, 2) are obtained. The energy transfer efficiency can be 23.05% when Yb^{3+} ions concentration is 1.0 mol%, while it can reach to 53.6% when Yb^{3+} ions concentration increases to 2.0 mol%, respectively.

3 Conclusions

In summary, the fabrication conditions and optical characteristics of Eu^{2+}-Yb^{3+} co-doped phosphate glass have been described. Eu^{3+} ions in the reducible effect of aluminium powder become divalent, while some of europium ions still exist as trivalent state. However, there is no effect for Eu^{3+} ions to change the NIR luminescence from Yb^{3+}. Excitation, emission and decay measurements are performed to prove the occurrence of cooperative energy transfer from one Eu^{2+} to two Yb^{3+} ions, which leads to 900～1100 nm near-infrared emission subsequently. From the decay curves, Inokuti-Hirayama′s model was used to analyze energy transfer mechanism between Eu^{2+} and Yb^{3+}, proving that the energy transfer of the electric dipole-dipole interaction is dominant in this system. The energy transfer efficiency is also calculated, which is 23.05% increased for the Eu^{2+}-1.0Yb^{3+} doped glass, and 53.6% increased for the Eu^{2+}-2.0Yb^{3+} doped glass compared with the same Eu^{2+} doped glass, respectively.

References

[1] ZHANG Q Y, YANG C H, JIANG Z H. Concentration-dependent near-infrared quantum cutting in $GdBO_3$: Tb^{3+}, Yb^{3+} nanosphosphors[J]. *Applied Physics Letters*, 2007, **90**(6): 061914.

[2] VERGEER P, VLUGT T J H, KOX M H F, *et al*. Quantum cutting by cooperative energy transfer in $Yb_xY_{1-x}PO_4$: Tb^{3+} [J]. *Physics Review B*, 2005, **71**: 014119.

[3] LIU Xiao-feng, YE Song, QIAO Yan-bo, *et al*. Cooperative

downconversion and near-infrared luminescence of Tb^{3+}-Yb^{3+} codoped lanthanum borogermanate glasses [J]. *Applied Physics B: Lasers and Optics*, 2009, **96**(1): 51-55.

[4] LAKSHMINARAYANA G, YANG Hu-cheng, YE Song, *et al*. Co-operative downconversion luminescence in Tm^{3+}/Yb^{3+} : SiO_2-Al_2O_3-LiF-GdF_3 glasses[J]. *Journal of Physics D: Applied Physics*, 2008, **41**: 175111.

[5] YE Song, ZHU Bin, LUO Jin, *et al*. Enhanced cooperative quantum cutting in Tm^{3+}-Yb^{3+} codoped glass ceramic containing LaF_3 nanocrystals[J]. *Optics Express*, 2008, **16**(12): 8989-8994.

[6] XIE Le-chun, WANG Yu-hua, ZHANG Hui-juan. Near-infrared quantum cutting in YPO_4 : Yb^{3+}, Tm^{3+} via cooperative energy transfer [J]. *Applied Physics Letters*, 2009, **94**(6): 061905-3.

[7] ZHANG Qiang, ZHU Bin, ZHUANG Yi-xi, *et al*. Quantum cutting in Tm^{3+}/Yb^{3+} codoped Lanthanum Aluminum Germanate glasses[J]. *Journal of American Ceramic Society*, 2010, **93**(3): 654-657.

[8] KATAYAMA Y, TANABE S. Near infrared downconversion in Pr^{3+}-Yb^{3+} codoped oxyfluoride glass ceramic[J]. *Optical Materials*, 2010, **33**(2): 176-179.

[9] ZHANG Q Y, YANG G F. Cooperative downconversion in $GdAl_3(BO_3)_4$: RE^{3+}, Yb^{3+} (RE = Pr, Tb, and Tm) [J]. *Applied Physics Letters*, 2007, **91**(5): 051903-3.

[10] ZHOU Jia-jia, ZHUANG Yi-xi, YE Song, *et al*. Broadband downconversion bansed infrared quantum cutting by cooperative energy transfer from Eu^{2+} to Yb^{3+} in glasses[J]. *Applied Physics Letters*, 2009, **95**(14): 141101-3.

[11] ZHOU Jia-jia, TENG Yu, LIN Geng, *et al*. Ultraviolet to near-infrared spectral modification in Ce^{3+} and Yb^{3+} codoped phosphate glasses[J]. *Journal of Non-Crystalline Solids*, 2011, **357**(11-13): 2336-2339.

[12] XIA Hai-ping, SONG Hong-wei, NIE Qiu-hua, *et al*. Preparation and optical spectroscopy of phosphate glasses containing divalent europium ions[J]. *Chinese Optics Letters*, 2003, **1**(5): 296-298.

[13] MURAKAMI S, HERREN M, RAU D, *et al*. Photoluminescence and decay profiles of undoped and Fe^{2+}, Eu^{3+} doped PLZT cearmic at low temperatures down to 10 K [J]. *Igorganica Chimica Acta*, 2000, 300-302: 1014-1021.

[14] ZHENG Yan-feng, CHEN Bao-jiu, ZHONG Haiyang, *et al*. Optical transition, excitation state absorption, and energy transfer study of Er^{3+}, Nd^{3+} single-doped, and Er^{3+}, Nd^{3+} codoped tellurite glasses for mid-infrared laser applications [J]. *Journal of American Ceramic Society*, 2011, **94**(6): 1766-1772.

· 下期预告 ·

空间遥感大气痕量气体临边探测仪设计与研究

薛庆生

(中国科学院长春光学精密机械与物理研究所, 长春 130033)

摘　要: 为满足空间大气痕量气体探测的迫切需求,设计并研制了一个空间遥感大气痕量气体临边探测仪原型样机. 该样机光学系统由离轴抛物面望远镜和改进型 Czerny-Turner 光谱仪组成,工作波段为 380～570 nm. 在工作波段内,点列图半径的均方根值均小于 9 μm,校正了像散,整个工作波段内同时获得了良好的成像质量. 原型样机质量 12 kg,体积 420×350×200 mm^3,空间像元分辨力 0.6 km,光谱分辨力 0.86 nm,各项指标均满足要求. 利用临边探测仪原型样机进行了外场观测试验,外场观测光谱数据与模拟光谱数据进行了比对,二者具有很好的一致性,表明大气痕量气体临边探测仪功能和性能良好,满足大气痕量气体探测的应用要求.

关键词: 光学设计; 成像光谱仪; 临边探测; 光谱分辨力; 空间分辨力